

Syntheses, Structures and Catalytic Properties of Two Mn(II) and Cd(II) Coordination Polymers through *in Situ* Ligand Reaction^①

ZHAO Su-Qin^{a②} GU Jin-Zhong^{b②}

^a (College of Physics and Electronic Information Engineering,
Qinghai University for Nationalities, Xining 810007, China)

^b (College of Chemistry and Chemical Engineering, Lanzhou University, Lanzhou 730000, China)

ABSTRACT Two coordination polymers, namely $[\text{Mn}(\mu\text{-Hcpia})(\text{bipy})(\text{H}_2\text{O})_2]_n$ (**1**) and $[\text{Cd}_3(\mu_3\text{-Hcpia})_2(\mu\text{-Hbiim})_2(\mu\text{-H}_2\text{biim})(\text{H}_2\text{O})_2]_n$ (**2**), have been constructed hydrothermally using H_2cbia (H_2cbia = 5-(4'-cyano-benzyloxy)isophthalic acid), bipy (bipy = 4,4'-bipyridine), H_2biim (H_2biim = 2,2'-biimidazole), and manganese or cadmium chlorides at 160 °C. Interestingly, the H_3cpia (H_3cpia = 5-(4'-carboxylphenoxy)isophthalic acid) ligand was generated by *in situ* hydrolysis of cyano group in H_2cbia . The products were isolated as stable crystalline solids and were characterized by IR spectra, elemental analyses, thermogravimetric analyses (TGA), and single-crystal X-ray diffraction analyses. Both compounds crystallize in the triclinic system, space group $P\bar{1}$. Compound **1** discloses a 1D linear chain of the **2C1** topological type. Adjacent chains are assembled into a 2D supramolecular sheet through O–H···O/N hydrogen bonds. Compound **2** features a 3D framework with a **3,4,4T25** topology. The luminescent and catalytic properties of two compounds were investigated. Compound **1** exhibits a superior catalytic activity in the cyanosilylation at room temperature.

Keywords: coordination polymer, tricarboxylic acid, luminescent properties, catalytic properties, *in situ* reaction; DOI: 10.14102/j.cnki.0254–5861.2011–3052

1 INTRODUCTION

During the past decades, the design and construction of functional coordination polymers have caught enormous attention of chemical researchers, not only because of their charming architectures and topologies, but also for their various potential applications in gas storage and separation, catalysis, magnetism, luminescence, and biomedicine^[1–12]. However, the design and composition of crystalline complexes with target structures as well as multifunction are of great important topics and are still the tremendous challenges because the assembly of coordination polymers is mainly affected by many factors, such as metal ions, organic and auxiliary ligands, metal-to-ligand ratio, solvent, and the reaction temperature^[13–22]. The metal ions and organic ligands are the key to get intriguing topologies and functional materials. Multicarboxylate ligands are frequently used for the construction of coordination polymers because they can

satisfy the charge-balance and provide diverse ligands and coordination modes^[5, 6, 14, 16, 17, 23, 24]. Among such polycarboxylate blocks, semirigid biphen ligands are particularly intriguing, since they enable the formation of uncommon metal-organic networks or even topologically unique nets; at the same time, such ligands can also show interesting properties along with flexibility and conformational diversity^[6, 14, 16, 17, 25].

In recent years, some *in situ* ligands or metal reactions have attracted increasing interest for the sake of obtaining new chemistry reactions, as well as the generation of novel coordination polymers^[26]. As we know, *in situ* ligand may contain three benefits: Firstly, *in situ* ligand synthesis produces the possibility of novel ligand and simultaneous metal coordination. Secondly, in some cases, *in-situ* ligand synthesis can be used as a simple and friendly synthesis route. Thirdly, *in situ* ligand synthesis has been used to gain ligands hard to obtain through assembly synthetic routes^[27, 28]. It is

Received 3 December 2020; accepted 8 February 2021 (CCDC 2023112 and 2023113 for **1** and **2**)

① This work was supported by the Science and Technology Plan of Qinghai Province (2020-ZJ-705)

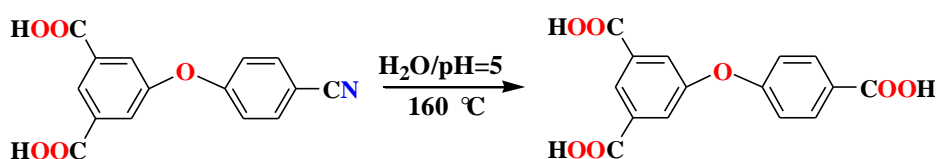
② Corresponding authors. E-mails: qzhshq@sina.com and gujzh@lzu.edu.cn

hard to access the ligands *in situ* reaction by conventional methods. Solvothermal (containing hydrothermal) method can be a good choice. Up to now, solvothermal-microwave as well as ultrasound method has been observed *in situ* reactions^[29].

Considering these in mind, recently, we have begun to construct coordination polymers by use of the advantages of *in situ* ligand reaction. On the basis of current research on *in situ* ligand reaction, the carboxylate-based ligands can be *in situ* generated from the CN-containing ligands precursor^[27, 30, 31]. Thus, the precursor we selected is 5-(4'-cyanobenzoxy)isophthalic acid (H₂cbia) due to its following

characteristics: (1) It contains two carboxylate and one CN groups, which can form a tricarboxylate ligand through *in situ* ligand reaction (Scheme 1); (2) Although its corresponding acid, 5-(4'-carboxylphenoxy)isophthalic acid (H₃cpia), has been applied in the construction of coordination polymers^[32-34], through *in situ* ligand reaction, novel coordination polymers possessing different structures with reported results may be generated.

Herein, we report the synthesis, crystal structures, luminescence and catalysis of Mn(II) and Cd(II) coordination polymers with H₃cpia ligands.



Scheme 1. H₃cpia ligand formed via the *in situ* reaction

2 EXPERIMENTAL

2.1 General procedures

All chemicals and solvents were of AR grade and used without further purification. Carbon, hydrogen and nitrogen were determined using an Elementar Vario EL elemental analyzer. IR spectra were recorded using KBr pellets and a Bruker EQUINOX 55 spectrometer. Thermogravimetric analysis (TGA) was performed under N₂ atmosphere with a heating rate of 10 K/min on a LINSEIS STA PT1600 thermal analyzer. Excitation and emission spectra were recorded on an Edinburgh FLS920 fluorescence spectrometer using the solid samples at room temperature. Powder X-ray diffraction patterns (PXRD) were measured on a Rigaku-Dmax 2400 diffractometer using CuK α radiation ($\lambda = 1.5406 \text{ \AA}$); the X-ray tube was operated at 40 kV and 40 mA. The data collection ranged from 5 ° to 45 °. Solution ¹H NMR spectra were recorded on a JNM ECS 400 M spectrometer.

2.2 Synthesis of compound 1

A mixture of MnCl₂·4H₂O (0.040 g, 0.2 mmol), H₂cbia (0.057 g, 0.2 mmol), bipy (0.031 g, 0.2 mmol), NaOH (0.016 g, 0.4 mmol), and H₂O (10 mL) was stirred at room temperature for 15 min, and then sealed in a 25 mL Teflon-lined stainless-steel vessel, and heated at 433 K for 3 days, followed by cooling to room temperature at a rate of 10 K h⁻¹. Yellow block-shaped crystals of **1** were isolated manually, and washed with distilled water. Yield: 55% (based

on H₂cbia). Anal. Calcd. (%) for C₂₅H₂₀MnN₂O₉: C, 54.86; H, 3.68; N, 5.12. Found (%): C, 55.02; H, 3.70; N, 5.09. IR (KBr, cm⁻¹): 3307m, 3092w, 1678w, 1612s, 1560s, 1502w, 1458w, 1414m, 1371s, 1318w, 1253w, 1168w, 1103w, 1072w, 1042w, 1002w, 976w, 910w, 853w, 814w, 782w, 730w, 680w, 624w. ν_{OH} 3307 and 3092, $\nu(\text{CO}_2\text{H})$ 1678, $\nu_{\text{as}}(\text{CO}_2)$ 1612 and 1560, $\nu_{\text{s}}(\text{CO}_2)$ 1414 and 1371.

2.3 Synthesis of compound 2

A mixture of CdCl₂·H₂O (0.040 g, 0.2 mmol), H₂cbia (0.057 g, 0.2 mmol), H₂biim (0.027 g, 0.2 mmol), NaOH (0.016 g, 0.4 mmol), and H₂O (10 mL) was stirred at room temperature for 15 min, and then sealed in a 25 mL Teflon-lined stainless-steel vessel, and heated at 433 K for 3 days, followed by cooling to room temperature at a rate of 10 K h⁻¹. Colourless block-shaped crystals of **2** were isolated manually, and washed with distilled water. Yield: 50% (based on H₂cbia). Anal. Calcd. (%) for C₄₈H₃₆Cd₃N₁₂O₁₆: C, 41.96; H, 2.64; N, 12.23. Found (%): C, 41.73; H, 2.65; N, 12.17. IR (KBr, cm⁻¹): 3442w, 3128w, 1664w, 1608m, 1565s, 1509w, 1453w, 1402s, 1369s, 1318w, 1258m, 1218w, 1171w, 1143w, 1107w, 1004w, 976w, 944w, 900w, 860w, 801w, 773w, 729w, 693w, 638w. ν_{OH} 3442 and 3128, $\nu(\text{CO}_2\text{H})$ 1664, $\nu_{\text{as}}(\text{CO}_2)$ 1608 and 1565, $\nu_{\text{s}}(\text{CO}_2)$ 1402 and 1369.

2.4 Structure determination

Two single crystals of the title compounds were mounted on a Bruker CCD diffractometer equipped with a graphite-monochromatic CuK α ($\lambda = 1.54178 \text{ \AA}$) radiation using a ϕ - ω

scan mode at 293(2) K. The structures were solved by direct methods with SHELXS-97^[35] and refined by full-matrix least-squares techniques on F^2 with SHELXL-97^[36]. All non-hydrogen atoms were refined anisotropically. All hydrogen atoms (except those bound to water molecules) were placed in the calculated positions with fixed isotropic thermal parameters and included in structure factor calculations in the final stage of full-matrix least-squares

refinement. The hydrogen atoms of water molecules were located by difference Fourier maps and constrained to ride on their parent O atoms. Detailed crystallographic data and structural refinements of compounds **1** and **2** are listed in Table 1. The selected important bond parameters are given in Table 2. The hydrogen bonds in crystal packing of compounds **1** and **2** are listed in Tables 3 and 4.

Table 1. Crystal Data and Structure Refinement for **1** and **2**

Compound	1	2
Formula	C ₂₅ H ₂₀ MnN ₂ O ₉	C ₄₈ H ₃₆ Cd ₃ N ₁₂ O ₁₆
Formula weight	547.37	1374.09
Crystal system	Triclinic	Monoclinic
Space group	$P\bar{1}$	$P\bar{1}$
a (Å)	9.9686(16)	10.1429(6)
b (Å)	10.6205(19)	11.5457(5)
c (Å)	12.053(2)	12.5340(5)
α (°)	87.932(16)	89.552(3)
β (°)	84.462(15)	73.329(4)
γ (°)	67.705(16)	70.864(5)
V (Å ³)	1175.2(4)	1322.38(12)
Z	2	1
D_c (g/cm ³)	1.547	1.725
μ (mm ⁻¹)	5.096	10.268
Independent reflections	3988	4577
R_{int}	0.0982	0.0232
$F(000)$	562	680
S	1.022	1.078
R, wR ($I > 2\sigma(I)$)	0.0781, 0.1038	0.0289, 0.0728

Table 2. Selected Bond Lengths (Å) and Bond Angles (°) for **1** and **2**

1							
Bond		Dist.		Bond		Dist.	
Mn(1)–O(1)		2.054(5)		Mn(1)–O(4) ⁱ		2.131(5)	
Mn(1)–O(9)		2.225(5)		Mn(1)–N(1)		2.245(6)	
Angle		(°)		Angle		(°)	
O(1)–Mn(1)–O(4) ⁱ		132.2(2)		O(1)–Mn(1)–O(8)		87.3(2)	
O(1)–Mn(1)–O(9)		90.2(2)		O(9)–Mn(1)–O(4) ⁱ		93.1(2)	
O(1)–Mn(1)–N(1)		138.4(2)		N(1)–Mn(1)–O(4) ⁱ		89.3(2)	
N(1)–Mn(1)–O(9)		90.3(2)					
Symmetry code: i: x–1, y, z							
2							
Bond		Dist.		Bond		Dist.	
Cd(1)–O(1)		2.495(3)		Cd(1)–O(2)		2.359(3)	
Cd(1)–O(8)		2.377(2)		Cd(1)–N(1)		2.388(3)	
Cd(2)–O(6) ⁱⁱⁱ		2.400(4)		Cd(2)–O(6) ^{iv}		2.400(4)	
Cd(2)–N(4) ^v		2.239(3)		Cd(2)–N(5)		2.342(3)	
Angle		(°)		Angle		(°)	
O(4) ⁱⁱ –Cd(1)–N(3)		136.74(10)		N(3)–Cd(1)–O(2)		86.87(10)	
O(8)–Cd(1)–N(3)		84.62(10)		O(4) ⁱⁱ –Cd(1)–O(8)		83.43(9)	
N(3)–Cd(1)–N(1)		96.27(10)		N(1)–Cd(1)–O(4) ⁱⁱ		93.06(10)	
N(1)–Cd(1)–O(8)		175.66(10)		N(3)–Cd(1)–O(1)		138.74(10)	
O(2)–Cd(1)–O(1)		53.57(9)		O(1)–Cd(1)–O(8)		86.62(9)	
N(4) ^v –Cd(2)–N(5)		104.64(11)		N(4)–Cd(2)–N(5)		75.36(11)	
N(4)–Cd(2)–O(6) ^{iv}		85.89(14)		N(5)–Cd(2)–O(6) ⁱⁱⁱ		79.50(14)	

Symmetry codes: ii: $x+1, y, z$; iii: $x, y+1, z-1$; iv: $-x+2, -y+2, -z$; v: $-x+2, -y+3, -z$

Table 3. Geometrical Parameters of Hydrogen Bonds for 1

D–H...A	d(D–H)/Å	d(H...A)/Å	d(D...A)/Å	∠DHA/°
O(7)–H(1)...O(3) ⁱ	0.85	2.05	2.895(9)	179
O(8)–H(1W)...O(3) ⁱⁱ	0.86	2.02	2.777(7)	146
O(8)–H(2W)...N(2) ⁱⁱⁱ	0.86	2.08	2.848(8)	148
O(9)–H(3W)...O(6) ^{iv}	0.89	1.99	2.834(8)	160
O(9)–H(4W)...O(2) ^v	0.88	1.87	2.738(7)	172

Symmetry codes: i: $-x+3, -y+2, -z$; ii: $-x+2, -y+2, -z+1$; iii: $-x+1, -y+1, -z+2$; iv: $-x+2, -y+2, -z$; v: $-x+2, -y+1, -z+1$

Table 4. Geometrical Parameters of Hydrogen Bonds for 2

D–H...A	d(D–H)/Å	d(H...A)/Å	d(D...A)/Å	∠DHA/°
O(7)–H(7)...N(5) ⁱ	0.82	2.59	3.324(7)	150
O(8)–H(1W)...O(4) ⁱⁱ	0.83	1.96	2.757(4)	159
O(8)–H(2W)...O(1) ⁱⁱⁱ	0.86	2.11	2.833(4)	142
N(2)–H(2)...O(2) ^{iv}	0.86	2.00	2.844(4)	167
N(6)–H(5)...O(3) ^v	0.86	1.93	2.781(4)	171

Symmetry codes: i: $x, y-1, z+1$; ii: $-x+1, -y+2, -z+1$; iii: $-x+2, -y+2, -z+1$; iv: $-x+2, -y+2, -z$; v: $x+1, y, z$

2.5 Catalytic cyanosilylation of aldehydes

In a typical test, a suspension of an aromatic aldehyde (0.50 mmol, 4-nitrobenzaldehyde as a model substrate), trimethylsilyl cyanide (1.0 mmol), and catalyst (typically 3 mol%) in dichloromethane (2.5 mL) was stirred at room temperature. After a desired reaction time, the catalyst was removed by centrifugation, followed by an evaporation of the solvent from the filtrate under reduced pressure to give a crude solid. This was dissolved in CDCl_3 and analyzed by ^1H NMR spectroscopy for quantification of products (Fig. 11). To perform the recycling experiment, the catalyst was isolated by centrifugation, washed with dichloromethane, dried at room temperature, and reused. The subsequent steps were performed as described above.

3 RESULTS AND DISCUSSION

3.1 Crystal structure of 1

X-ray crystallography analysis reveals that compound 1 crystallizes in the triclinic system space group $P\bar{1}$. As shown

in Fig. 1, the asymmetric unit of 1 bears one crystallographically unique Mn(II) atom, one $\mu\text{-Hcpia}^{2-}$ block, one bipy moiety, and two H_2O ligands. The five-coordinated Mn(1) atom exhibits a distorted trigonal bipyramidal $\{\text{MnNO}_4\}$ environment, which is occupied by two carboxylate O donors from two different $\mu\text{-Hcpia}^{2-}$ blocks, two O atoms from two H_2O ligands, and one N atom from the bipy moiety. The Mn–O and Mn–N bond distances are 2.054(5)–2.225(5) and 2.245(6) Å, respectively; these are within the normal ranges observed in related Mn(II) compounds^[14, 17]. In 1, the Hcpia^{2-} ligand adopts the coordination mode I (Scheme 2) with two COO^- groups being monodentate. In the Hcpia^{2-} ligand, a dihedral angle (between two aromatic rings) and a $\text{C–O}_{\text{ether}}\text{–C}$ angle are 81.08 and 118.26°, respectively. The bipy moiety takes a terminal coordination mode (mode III, Scheme 2). The $\mu\text{-Hcpia}^{2-}$ ligands connect Mn atoms to give a 1D linear chain of the 2C1 topological type (Figs. 2 and 3). Adjacent chains are assembled into a 2D supramolecular sheet through $\text{O–H}\cdots\text{O/N}$ hydrogen bonds (Fig. 4).

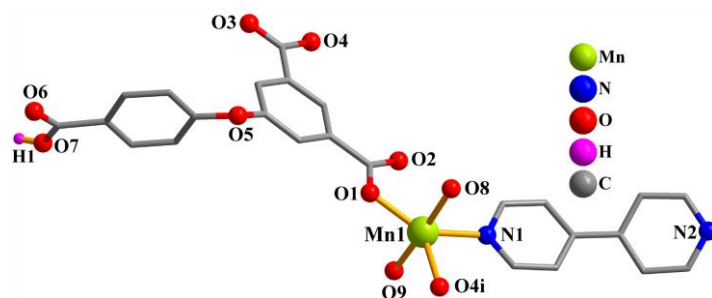


Fig. 1. Coordination environments of the Mn(II) atom in compound 1.

The hydrogen atoms are omitted for clarity except in COOH group (Symmetry code: i: $x-1, y, z$)

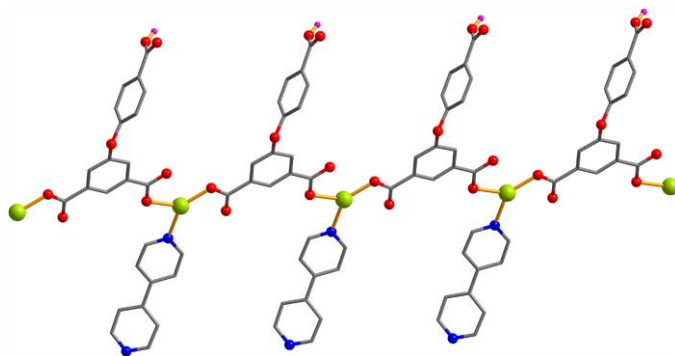


Fig. 2. Perspective view of the 1D chain along the *b* axis. The H₂O ligands are omitted for clarity

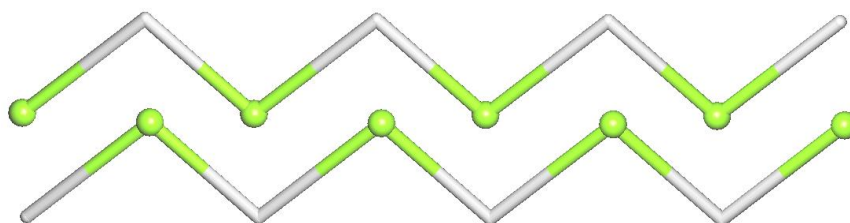


Fig. 3. Topological representation of two 1D chains in 1 with the 2C1 topology; Mn centers (green balls), centroids of μ -Hcpia²⁻ linkers (gray). View along the *b* axis

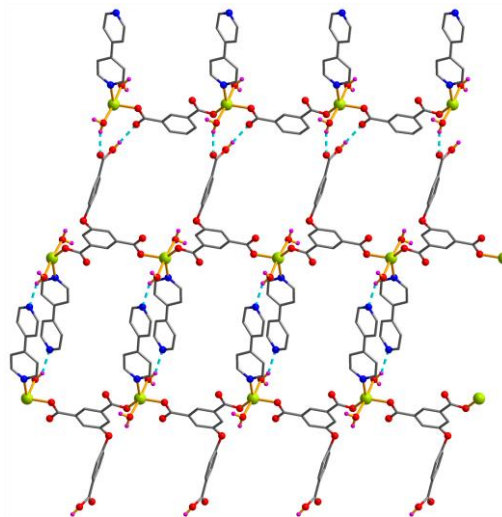
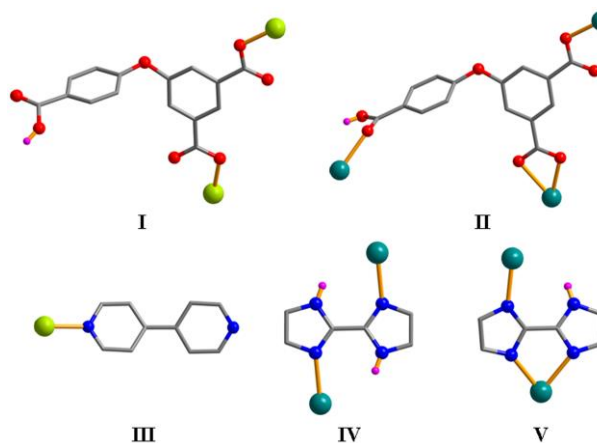


Fig. 4. Perspective view of the 2D sheet along the *ac* plane. Dashed lines present the hydrogen bonds



Scheme 2. Coordination modes of the Hcpia²⁻, bipy and H₂biim/Hbiim⁻ ligands in compounds 1 and 2

3.2 Crystal structure of 2

The asymmetric unit of compound **2** contains two crystallographically unique Cd(II) atoms (Cd(1) with full occupancy and Cd(2) with half occupancy), one μ_3 -Hcpia²⁻ block, one Hbiim⁻ moiety, a half of H₂biim, and one H₂O ligand. As depicted in Fig. 5, the six-coordinate Cd(1) atom features a distorted octahedral {CdN₂O₄} environment, which is filled by three carboxylate O atoms from two μ_3 -Hcpia²⁻ blocks, one O donor from the H₂O ligand, one N atom from the H₂biim, and one N atom of one Hbiim⁻ moiety. The Cd(2) center is also six-coordinated and displays a distorted octahedral {CdN₄O₂} geometry. It is taken by two carboxylate O atoms from two μ_3 -Hcpia²⁻ blocks and four N donors from two Hbiim⁻ ligands. The bond lengths of Cd–O are in the 2.230(2)~2.495(3) Å range, while the Cd–N bonds are 2.226(3)~2.388(3) Å, being comparable to those found in some reported Cd(II) compounds^[14, 25, 28]. In **2**, the Hcpia²⁻

block acts as a μ_3 -linker (mode II, Scheme 2), in which three carboxylate groups adopt monodentate or bidentate modes. Besides, the μ_3 -Hcpia²⁻ ligand is considerably bent, showing a dihedral angle of 68.14 ° (between two aromatic rings) and the C–O_{ether}–C angle of 120.67 °. The H₂biim and Hbiim⁻ moieties exhibit a μ -bridging coordination mode (modes IV and V, Scheme 2). The μ_3 -Hcpia²⁻, μ -H₂biim and μ -Hbiim⁻ ligands multiply connect Cd(II) centers to form a 3D framework (Fig. 6). The 3D metal-organic framework is assembled from the 4-connected Cd(1)/Cd(2) nodes, 3-connected μ_3 -Hcpia²⁻ blocks, 2-connected μ -H₂biim and μ -Hbiim⁻ linkers. As a result, a complex trinodal 3,4,4-connected net with a **3,4,4T25** topology^[37-39] is generated (Fig. 7). The network is described by a point symbol of (6².8⁴)(6³)₂(6⁴.8²)₂, wherein the (6².8⁴), (6³), and (6⁴.8²)₂ notations correspond to Cd2, μ_3 -Hcpia²⁻, and Cd1 nodes, respectively.

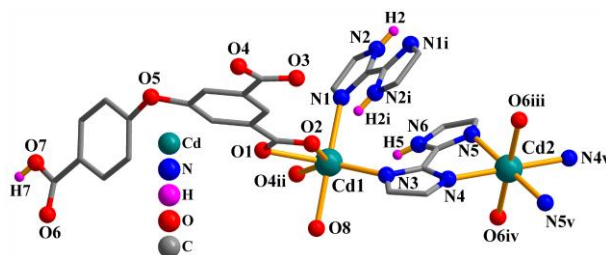


Fig. 5. Coordination environments of the Cd(II) atoms. The hydrogen atoms are omitted for clarity except in COOH and NH groups (Symmetry codes: i: $-x+2, -y+2, -z$; ii: $x+1, y, z$; iii: $x, y+1, z-1$; iv: $-x+2, -y+2, -z$; v: $-x+2, -y+3, -z$)

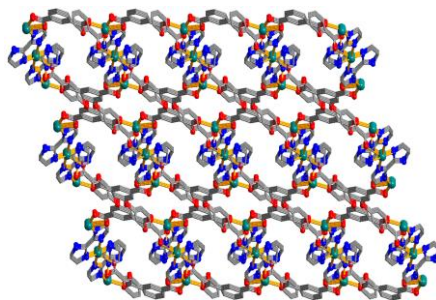


Fig. 6. View of 3D metal-organic framework along the *ac* plane. The H₂O ligands are omitted for clarity

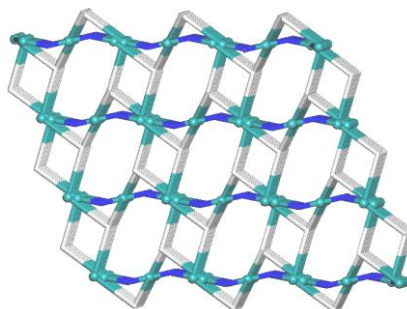


Fig. 7. Topological representation of a trinodal 3,4,4-connected metal-organic framework in **2** with the **3,4,4T25** topology; view along the *b* axis; 4-connected Cd nodes (turquoise balls), centroids of 3-connected μ_3 -Hcpia²⁻ blocks (gray), centroids of 2-connected μ -H₂biim and μ -Hbiim⁻ linkers (blue). View of 3D metal-organic framework along the *ac* plane. The H₂O ligands are omitted for clarity

3.3 Thermal analysis

To determine the thermal stability of polymers **1** and **2**, their thermal behaviors were investigated under nitrogen atmosphere by thermogravimetric analysis (TGA). As shown in Fig. 8, compound **1** loses its two coordinated water

molecules in the 413~473 K range (exptl, 6.4%; calcd. 6.6%), followed by the decomposition at 485 K. For **2**, one weight loss (exptl, 2.4%; calcd. 2.6%) in the 449~508 K region corresponds to a removal of two H₂O ligands; decomposition of the sample occurs only at 561 K.

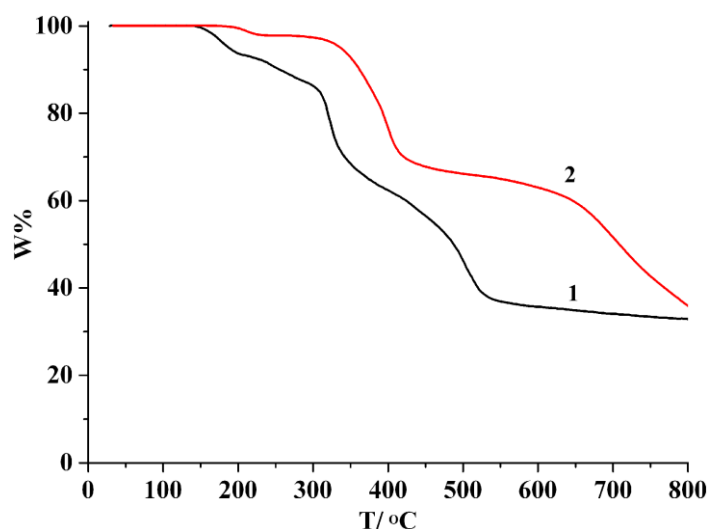


Fig. 8. TGA curves of compounds **1** and **2**

3.4 Luminescent properties

The excitation and emission spectra of 5-(4'-cyanobenzoxy)isophthalic acid (H₂cbia) and polymer **2** were measured in the solid state at room temperature (Figs. 9 and 10). The uncoordinated H₂cbia shows a weak photoluminescence with an emission maximum at 404 nm ($\lambda_{\text{ex}} = 320$ nm). In contrast, compound **2** displays the significantly more intense emission

bands with the maxima at 379 nm ($\lambda_{\text{ex}} = 320$ nm), respectively. All bands can be assigned to the intraligand ($\pi^* \rightarrow n$ or $\pi^* \rightarrow \pi$) emission^[14, 17]. The luminescence enhancement in the coordination compounds can be attributed to the binding of ligands to the metal centers, which effectively increases the rigidity of the ligand and reduces the loss of energy by radiationless decay^[25, 28].

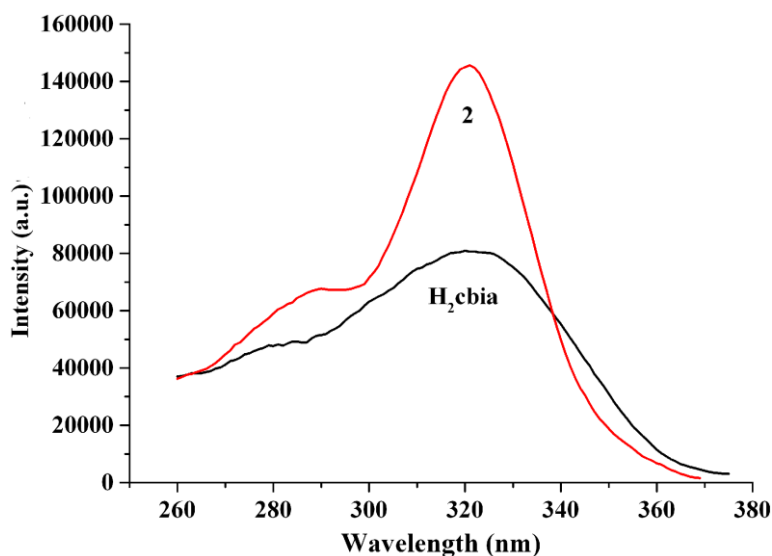
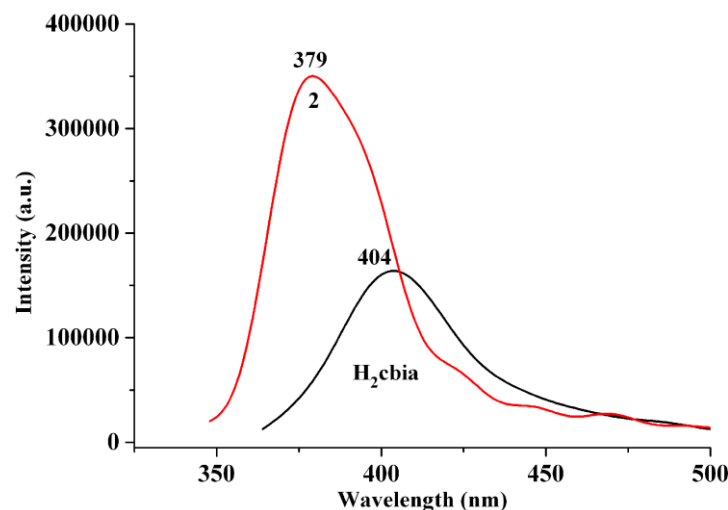


Fig. 9. Solid-state excitation spectra of H₂cbia and compound **2** at room temperature

Fig. 10. Solid-state emission spectra of H₂cbia and compound 2 at room temperature

3.5 Catalytic cyanosilylation of aldehydes

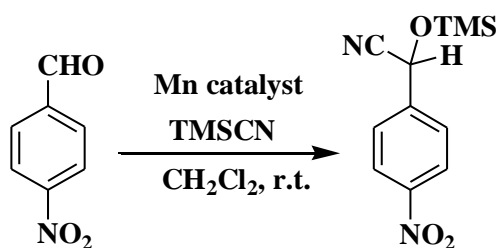
Given the potential of manganese(II) and cadmium(II) coordination compounds to catalyze the organic reactions^[40-42], we explored the application of **1** and **2** as heterogeneous catalysts in the cyanosilylation of 4-nitrobenzaldehyde as a model substrate to give 2-(4-nitrophenyl)-2-[(trimethylsilyl)oxy]acetonitrile. Typical tests were carried

out by reacting a mixture of 4-nitrobenzaldehyde, trimethylsilyl cyanide (TMSCN), and a Mn or Cd catalyst in dichloromethane at room temperature (Scheme 3, Table 5). Such effects as reaction time, catalyst loading, solvent composition, catalyst recycling, and finally substrate scope were investigated

Table 5. Mn and Cd-Catalyzed Cyanosilylation of 4-Nitrobenzaldehyde with TMSCN

Entry	Catalyst	Time, h	Catalyst loading, mol%	Solvent	Yield ^a , %
1	1	1	3.0	CH ₂ Cl ₂	37
2	1	2	3.0	CH ₂ Cl ₂	59
3	1	4	3.0	CH ₂ Cl ₂	67
4	1	6	3.0	CH ₂ Cl ₂	74
5	1	8	3.0	CH ₂ Cl ₂	79
6	1	10	3.0	CH ₂ Cl ₂	83
7	1	12	3.0	CH ₂ Cl ₂	87
8	1	12	2.0	CH ₂ Cl ₂	68
9	1	12	4.0	CH ₂ Cl ₂	89
10	1	12	3.0	CH ₃ CN	75
11	1	12	3.0	THF	69
12	1	12	3.0	CH ₃ OH	79
13	1	12	3.0	CH ₃ Cl	65
14	2	12	3.0	CH ₂ Cl ₂	42
15	Blank	12	-	CH ₂ Cl ₂	2
16	MnCl ₂	12	3.0	CH ₂ Cl ₂	5
17	H ₃ cpia	12	3.0	CH ₂ Cl ₂	3

^a Calculated by ¹H NMR spectroscopy: mol(product)/mol(aldehyde)×100



Scheme 3. Mn-catalyzed cyanosilylation of 4-nitrobenzaldehyde (model substrate)

Upon using compound **1** as the catalyst (3 mol-%), a high conversion of 87% of 4-nitrobenzaldehyde into 2-(4-nitrophenyl)-2-[(trimethylsilyl)oxy]acetonitrile was reached

after 12 h in dichloromethane at room temperature (Table 5, entry 7).

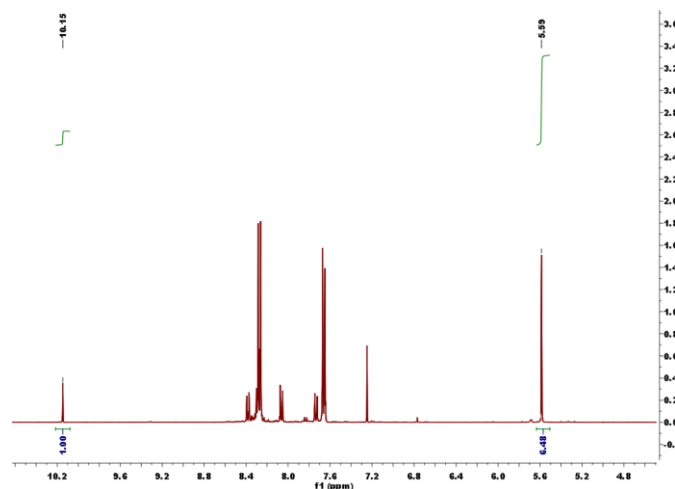


Fig. 11. Example of integration in the ^1H -NMR spectrum for the determination of cyanosilylation reaction products (Table 5, Entry 7)

The results show that compound **1** is more active than **2**. Although a relationship between structure and catalytic activity in the present study can not be clearly established, the highest conversion shown by compound **1** may eventually be associated to its 1D structure for easily accessible metal centers, together with the higher Lewis acidity of the manganese sites^[43].

We also compared the activities of catalyst **1** in the reactions of other substituted aromatic and aliphatic aldehydes with trimethylsilyl cyanide, and the corresponding

cyanohydrin derivatives were produced in yields ranging from 66 to 81% (Table 6). Aryl aldehydes bearing strong electron-withdrawing substituents (e.g., nitro and chloro) exhibited the higher reactivities (Table 6, entries 2~5), which may be related to an increase in the electrophilicity of the substrate. Aldehydes containing electron-donating groups (e.g., methyl) showed lower reaction yields (Table 6, entry 7), as expected. An ortho-substituted aldehyde showed lower reactivity, possibly as a result of steric hindrance.

Table 6. Cyanosilylation of Various Aldehydes with TMSCN Catalyzed by **1**

Entry	Substituted benzaldehyde substrate ($\text{R}-\text{C}_6\text{H}_4\text{CHO}$)	Product yield ^a , %
1	R = H	69
2	R = 2- NO_2	75
3	R = 3- NO_2	81
4	R = 4- NO_2	87
5	R = 4-Cl	78
6	R = 4-OH	74
7	R = 4- CH_3	66

^a Calculated by ^1H NMR spectroscopy: $\text{mol}(\text{product})/\text{mol}(\text{aldehyde}) \times 100$

To examine the stability of **1** in the cyanosilylation reaction, we tested the recyclability of this heterogeneous catalyst. For this purpose, upon completion of a reaction cycle, we separated the catalyst by centrifugation, washed it with CH_2Cl_2 , and dried it at room temperature before further use. We repeated recycled catalyst **1**, and the catalytic system

maintained the higher activity over at least five consecutive cycles (the yields are 85, 85, 83, and 82% for the second to fifth run, respectively). According to the PXRD data (Fig. 12), the structure of **1** is essentially preserved after five catalytic cycles.

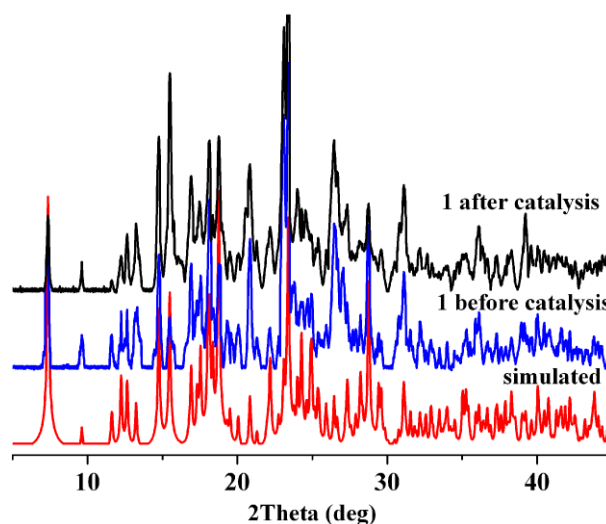


Fig. 12. PXRD patterns for 1: simulated (red), before (blue) and after (black) catalysis

4 CONCLUSION

In summary, we have synthesized two Mn(II) and Cd(II) coordination polymers based on an tricarboxylate ligand generated *in situ* reaction. Compound 1 discloses a 1D chain structure, which is assembled to a 2D supramolecular

network through O–H···O/N hydrogen bonds. Compound 2 features a 3D framework with a **3,4,4T25** topology. The luminescent and catalytic properties of both compounds were investigated. Compound 1 revealed a superior catalytic activity in the cyanosilylation at room temperature.

REFERENCES

- (1) Yu, L.; Dong, X. L.; Gong, Q. H.; Acharya, S. R.; Lin, Y. H.; Wang, H.; Han, Y.; Thonhauser, T.; Li, J. Splitting mono- and dibranched alkane isomers by a robust aluminium-based metal-organic framework material with optimal pore dimensions. *J. Am. Chem. Soc.* **2020**, 142, 6925–6929.
- (2) Fan, W. D.; Yuan, S.; Wang, W. J.; Feng, L.; Liu, X. P.; Zhang, X. R.; Wang, X.; Kang, Z. X.; Dai, F. N.; Yuan, D. Q.; Sun, D. F.; Zhou, H. C. Optimizing multivariate metal-organic frameworks for efficient C₂H₂/CO₂ separation. *J. Am. Chem. Soc.* **2020**, 142, 8728–8737.
- (3) Wang, H.; Li, J. Microporous metal-organic frameworks for adsorptive separation of C5–C6 alkane isomers. *Acc. Chem. Res.* **2019**, 52, 1968–1978.
- (4) Xiao, J. D.; Jiang, H. L. Metal-organic frameworks for photocatalysis and photothermal catalysis. *Acc. Chem. Res.* **2019**, 52, 356–366.
- (5) Gu, J. Z.; Wen, M.; Cai, Y.; Shi, Z. F.; Arol, A. S.; Kirillova, M. V.; Kirillov, A. M. Metal-organic architectures assembled from multifunctional polycarboxylates: hydrothermal self-assembly, structures, and catalytic activity in alkane oxidation. *Inorg. Chem.* **2019**, 58, 2403–2412.
- (6) Gu, J. Z.; Wen, M.; Cai, Y.; Shi, Z. F.; Nesterov, D. S.; Kirillova, M. V.; Kirillov, A. M. Cobalt(II) coordination polymers assembled from unexplored pyridine-carboxylic acids: structural diversity and catalytic oxidation of alcohols. *Inorg. Chem.* **2019**, 58, 5875–5885.
- (7) Roy, M.; Adhikary, A.; Mondal, A. K.; Mondal, R. Multifunctional properties a 1D helical Co(II) coordination polymers: toward single-ion magnetic behavior and efficient dye degradation. *ACS Omega* **2018**, 3, 15315–15324.
- (8) Salitros, I.; Herchel, R.; Fuhr, O.; Gonzalez-Prieto, R.; Ruben, M. Polynuclear iron(II) complexes with 2,6-bis(pyrazol-1-yl)-pyridineanthracene ligands exhibiting highly distorted high-spin centers. *Inorg. Chem.* **2019**, 58, 4310–4319.
- (9) Lustig, W. P.; Mukherjee, S.; Rudd, N. D.; Desai, A. V.; Li, J.; Ghosh, S. K. Metal-organic frameworks: functional luminescent and photonic materials for sensing applications. *Chem. Soc. Rev.* **2017**, 46, 3242–3285.
- (10) Cui, Y. J.; Yue, Y. F.; Qian, G. D.; Chen, B. L. Luminescent functional metal-organic frameworks. *Chem. Rev.* **2012**, 112, 1126–1162.
- (11) Haddad, S.; Lázaro, I. A.; Fantham, M.; Mishra, A.; Silvestre-Albero, J.; Osterrieth, J. W. M.; Schierle, G. S. K.; Kaminski, C. F.; Forgan, R. S.; Fairen-Jimenez, D. Design of a functionalized metal-organic framework system of enhanced targeted delivery to mitochondria. *J. Am. Chem. Soc.* **2020**, 142, 6661–6674.
- (12) Cai, H.; Huang, Y. L.; Li, D. Biological metal-organic frameworks: structures, host-guest chemistry and bio-applications. *Coord. Chem. Rev.* **2019**, 378, 207–221.

- (13) Liu, J. J.; Lu, Y. W.; Lu, W. B. Metal-dependent photosensitivity of three isostructural 1D CPs based on the 1,1'-bis(3-carboxylatobenzyl)-4,4'-bipyridinium moiety. *Dalton Trans.* **2020**, 49, 4044–4049.
- (14) Gu, J. Z.; Cui, Y. H.; Liang, X. X.; Wu, J.; Lv, D. Y.; Kirillov, A. M. Structurally distinct metal-organic and H-bonded networks derived from 5-(6-carboxypyridin-3-yl)isophthalic acid: coordination and template effect of 4,4'-bipyridine. *Cryst. Growth Des.* **2016**, 16, 4658–4670.
- (15) Han, S. D.; Chen, Y. Q.; Zhao, J. P.; Liu, S. J.; Miao, X. H.; Hu, T. L.; Bu, X. H. Solvent-induced structural diversities from discrete cup-shaped Co₈ clusters to Co₈ cluster-based chains accompanied by a situ ligand conversion. *CrystEngComm*. **2014**, 16, 753–756.
- (16) Zou, X. Z.; Wu, J.; Gu, J. Z.; Zhao, N.; Feng, A. S.; Li, Y. Syntheses of two nickel(II) coordination compounds based on a rigid linear tricarboxylic acid. *Chin. J. Inorg. Chem.* **2019**, 35, 1705–1711.
- (17) Gu, J. Z.; Gao, Z. Q.; Tang, Y. pH and auxiliary ligand influence on the structural variations of 5(2'-carboxylphenyl) nicotinate coordination polymers. *Cryst. Growth Des.* **2012**, 12, 3312–3323.
- (18) Li, Y.; Wu, J.; Gu, J. Z.; Qiu, W. D.; Feng, A. S. Temperature-dependent syntheses of two manganese(II) coordination compounds based on an ether-bridged tetracarboxylic acid. *Chin. J. Struct. Chem.* **2020**, 39, 727–736.
- (19) Zhang, J.; Liang, J. X.; Wang, Y.; Zhai, L. J.; Niu, X. Y.; Huo, T. P. Synthesis and electrochemical properties of temperature-induced two metal-organic frameworks-based electrodes for supercapacitor. *Cryst. Growth Des.* **2020**, 20, 460–467.
- (20) Hou, Y. L.; Peng, Y. L.; Diao, Y. X.; Liu, J.; Chen, L. Z.; Li, D. Side chain induced self-assembly and selective catalytic oxidation activity of copper(I)-copper(II)-N₄ complexes. *Cryst. Growth Des.* **2020**, 20, 1237–1241.
- (21) Phukan, N.; Goswami, S.; Lipstman, S.; Goldberg, I.; Tripuramallu, B. K. Solvent influence in obtaining diverse coordination symmetries of Dy(III) metal centers in coordination polymers: synthesis, characterization, and luminescent properties. *Cryst. Growth Des.* **2020**, 20, 2973–2984.
- (22) Rosa, I. M. L.; Costa, M. C. S.; Vitto, B. S.; Amorim, L.; Correa, C. C.; Pinheiro, C. B.; Doriguetto, A. C. Influence of synthetic methods in the structure and dimensionality of coordination polymers. *Cryst. Growth Des.* **2016**, 16, 1606–1616.
- (23) Grape, E. S.; Xu, H. Y.; Cheung, O.; Calmels, M.; Zhao, J. J.; Dejoie, C.; Proserpio, D. M.; Zou, X. D.; Inge, A. K. Breathing metal-organic framework based on flexible inorganic building units. *Cryst. Growth Des.* **2020**, 20, 320–329.
- (24) Ge, Y. F.; Teng, B. S.; Lv, L. L.; Chen, R.; Wu, B. L. Homochiral metal-organic frameworks of lead(II) and cadmium(II) constructed by amino acid-functionalized isophthalic acids: synthesis, structure diversity, and optical properties. *Cryst. Growth Des.* **2020**, 20, 486–497.
- (25) Gu, J. Z.; Cai, Y.; Wen, M.; Shi, Z. F.; Kirillov, A. M. A new series of Cd(II) metal-organic architectures driven by soft ether-bridged tricarboxylate spacers: synthesis, structural and topological versatility, and photocatalytic properties. *Dalton Trans.* **2018**, 47, 14327–14339.
- (26) Wang, Q.; Fan, Y.; Song, T. Y.; Xu, J. N.; Wang, J.; Chai, J.; Liu, Y. L.; Wang, L. Zhang, L. R. *In situ* synthesis of a series of lanthanide coordination polymers based on *N*-heterocyclic carboxylate ligands: crystal structure and luminescence. *Inorg. Chim. Acta* **2015**, 438, 128–134.
- (27) Li, Y. Y.; Lu, Y. Q.; Qiao, X. Y.; Huang, W. M.; Niu, Y. Y. *In situ* formation of 4-cyanopyridinecarboxylic acid and its polyacid doping coordination polymer for adsorption of organic dyes in wastewater. *Inorg. Chem. Commun.* **2020**, 118, 108002.
- (28) Wilson, J. A.; Uebler, J. W.; LaDuca, R. L. Cadmium adipate coordination polymers prepared with isomeric pyridylamide precursors: pH-dependent *in situ* reaction chemistry and divergent dimensionalities. *CrystEngComm*. **2013**, 15, 5218–5225.
- (29) Zhong, D. C.; Guo, H. B.; Deng, J. H.; Chen, Q.; Luo, X. Z. Two coordination polymers of benzene-1,2,4,5-tetracarboxylic acid (H₄BTC): *in situ* ligand syntheses, structures, and luminescent properties. *CrystEngComm*. **2015**, 17, 3519–3525.
- (30) Hu, T. P.; Bi, W. H.; Hu, X. Q.; Zhao, X. L.; Sun, D. F. Construction of metal-organic frameworks with novel {Zn₈O₁₃} SBU or chiral channels through *in situ* ligand reaction. *Cryst. Growth Des.* **2010**, 10, 3324–3326.
- (31) Evans, O. R.; Xiong, R. G.; Wang, Z. Y.; Wong, G. K.; Lin, W. B. Crystal engineering of acentric diamondoid metal-organic coordination networks. *Angew. Chem. Int. Ed.* **1999**, 38, 536–538.
- (32) Mishra, R.; Ahmad, M.; Tripathi, M. R.; Butcher, R. J. Four novel coordination polymers of transition metals built using a semi rigid oxygen donor ligand: crystal structures, novel topology and emission studies. *Polyhedron* **2013**, 50, 169–178.
- (33) Lama, P.; Aijaz, A.; Sañudo, E. C.; Bharadwaj, P. K. Synthesis, structure, and magnetic properties of cobalt(II) coordination polymers from a new tripodal carboxylate ligand: weak ferromagnetism and metamagnetism. *Cryst. Growth Des.* **2010**, 10, 283–290.
- (34) Zhang, X.; Ma, G. C.; Kong, F. Z.; Yu, Z. Y.; Wang, R. H. A two-fold interpenetrating metal-organic framework based on tetranuclear zinc-carboxylate clusters. *Inorg. Chem. Commun.* **2012**, 22, 44–47.
- (35) Sheldrick, G. M. *SHELXS 97, Program for Solution of Crystal Structure*. University of Göttingen, Germany **1997**.
- (36) Sheldrick, G. M. *SHELXL 97, Program for Refinement of Crystal Structure*. University of Göttingen, Germany **1997**.

- (37) Shi, Z. Z.; Pan, Z. R.; Jia, H. L.; Chen, S. G.; Qin, L.; Zheng, H. G. Zn(II)/Cd(II) terephthalate coordination polymers incorporating bi-, tri-, and tetra-topic phenylamine derivatives: crystal structures and photoluminescent properties. *Cryst. Growth Des.* **2016**, 16, 2747–2755.
- (38) Yang, R.; Liu, Y. G.; Van Hecke, K.; Cui, G. H. Synthesis and characterization of two cobalt(II) coordination polymers based on 5-tert-butyl isophthalic acid and bis(benzimidazole) ligands. *Transit. Metal Chem.* **2015**, 40, 333–340.
- (39) Qin, L.; Zheng, X. H.; Xiao, S. L.; Cui, G. H. Two cobalt(II) complexes based on a flexible bis(5,6-dimethylbenzimidazole) and rigid organic dicarboxylate ligands. *Transit. Metal Chem.* **2013**, 38, 891–897.
- (40) Loukopoulos, E.; Kostakis, G. E. Recent advances of one-dimensional coordination polymers as catalysts. *J. Coord. Chem.* **2018**, 71, 371–410.
- (41) Pal, S.; Maiti, S.; Nayek, H. P. A three-dimensional (3D) manganese (II) coordination polymer: synthesis, structure and catalytic activities. *Appl Organometal Chem.* **2018**, 32, 4447.
- (42) Gupta, V.; Mandal, S. K. Coordination driven self-assembly of [2+2+2] molecular squares: synthesis, crystal structures, catalytic and luminescence properties. *Dalton Trans.* **2018**, 47, 9742–9754.
- (43) Karmakar, A.; Paul, A.; Rubio, G. M. D. M.; Guedes da Silva, M. F. C.; Pombeiro, A. J. L. Zinc(II) and copper(II) metal-organic frameworks constructed from a terphenyl-4,4''-dicarboxylic acid derivative: synthesis, structure, and catalytic application in the cyanosilylation of aldehydes. *Eur. J. Inorg. Chem.* **2016**, 5557–5567.